

GaN-based LED structures on selectively grown semi-polar crystal facets

Ferdinand Scholz^{*1}, Thomas Wunderer¹, Martin Feneberg², Klaus Thonke², Andrei Chuvilin³, Ute Kaiser³, Sebastian Metzner⁴, Frank Bertram⁴, and Jürgen Christen⁴

¹Institute of Optoelectronics, Ulm University, 89069 Ulm, Germany

²Institute of Semiconductor Physics, Ulm University, 89069 Ulm, Germany

³Central Facility of Electron Microscopy, Ulm University, 89069 Ulm, Germany

⁴Institute of Experimental Physics, Otto von Guericke University, 39106 Magdeburg, Germany

Received 8 October 2009, revised 8 December 2009, accepted 9 December 2009

Published online 17 May 2010

Keywords growth, GaInN, LEDs, morphology, selective area epitaxy

* Corresponding author: e-mail ferdinand.scholz@uni-ulm.de, Phone: +49-731-5026052, Fax: +49-731-5026049

In conventional nitride-based light emitting diodes, huge internal electric fields lead to a reduced overlap of electron and hole wave functions in the active GaInN quantum wells as a consequence of the piezoelectricity of these polar materials. In order to minimize these internal fields while still maintaining the well-established c-direction as main epitaxial growth direction for high-quality low-defect-density layers, we have investigated semi-polar LED structures on the side-facets of triangular GaN stripes grown by selective area epitaxy. The reduced

internal electric field could be confirmed by several spectroscopic methods. We found a strongly facet dependent growth mechanism leading to very flat surfaces on $\{1\bar{1}01\}$ facets as opposed to their $\{11\bar{2}2\}$ counterparts. An increased indium uptake on semipolar $\{1\bar{1}01\}$ facets as compared to conventional c-plane layers helped to shift the LED emission to longer wavelengths beyond 500 nm in the green spectral range despite the significantly reduced field-dependent Stark shift.

© 2010 WILEY-VCH Verlag GmbH & Co. KGaA, Weinheim

1 Introduction Optoelectronic devices working in the short wavelength region of the visible spectrum have seen a tremendous development over the past 15 years since basic material issues of GaN and its related alloys like heteroepitaxy on foreign substrates and p-doping could be mastered. However, green light emitters still have substantially lower quantum efficiencies and worse performance than their blue counterparts. This is closely related to the intrinsic properties of GaInN with higher In-content as needed for such long wavelength applications. In particular, two main problems have been identified: First, $\text{Ga}_{1-x}\text{In}_x\text{N}$ with In contents x exceeding about 10% shows increasing composition fluctuations making its optoelectronic properties more and more unsuitable for high-efficiency LEDs and laser diodes. This is mainly caused by the phase diagram of GaInN, which contains a miscibility gap [1, 2], although it is not yet completely understood how this result from equilibrium thermodynamics is applicable in epitaxial methods like metalorganic vapor phase epitaxy (MOVPE) or molecular beam epitaxy (MBE) which are mostly non-equilibrium processes. Moreover, GaInN needs comparably

low growth temperatures due to the unfavorable vapor pressure of In over the compound, which hampers a defect-free epitaxial growth. Second, due to the different lattice constants between the GaInN active quantum wells and the surrounding (Al)GaN layers, the quantum wells are compressively strained. When grown in the most common c-direction, this biaxial strain gives rise to strong internal piezoelectric fields [3], which lead to a local separation of electrons and holes in these quantum wells due to the quantum confined Stark effect (QCSE). Owing to the reduced overlap of the electron and hole wave function, their recombination probability decreases making longer wavelength device structures less efficient.

The latter problem can be reduced by redirecting the biaxial strain to other planes than the generally used (0001) crystal plane (c-plane) [4], which leads to non- or semipolar heterostructures, where the piezoelectric fields decrease substantially or even vanish. Several different approaches are currently studied to realize such non- or semi-polar device structures. Best results including laser diodes emitting at 530 nm [5] have been reported for device

structures grown on non- or semipolar bulk substrates. Such substrates are cut from thick polar GaN wafers grown by hydride vapor phase epitaxy to a thickness of several millimeters [6]. However, this thickness limits the areal size of the non- or semipolar substrates to values of typically few centimeters by some millimeters making them exceptionally expensive and not suitable for device mass production.

Other approaches are using specifically oriented foreign substrates like r-plane sapphire or m-plane SiC, on which non-polar a-plane or m-plane GaN can be grown, respectively. Even more exotic substrates like LiAlO₂ [7] have been proposed, on which pure m-plane GaN {1 $\bar{1}$ 00} growth has been achieved. However, up to now the GaN layer quality on these substrates cannot compete with that obtained on the commonly used c-plane sapphire or SiC wafers. Typically, high densities of stacking faults and other crystalline defects evolve dominating completely the optoelectronic properties of these epitaxial layers and are made responsible for the inferior performance of respective light emitting devices.

These problems may be overcome by starting the epitaxial growth in the c-direction, but forming GaN stripes by selective area epitaxy where other crystal planes develop on the stripe facets, on which eventually the GaInN-GaN structures can be grown [8–11]. Depending on the stripe orientation and the growth conditions, different crystal facets can be prepared [12] which possess reduced or even zero polarization fields. We have concentrated our studies on stripes with triangular cross-section, i.e. only one semi-polar facet type develops in either stripe direction. Such structures can be embedded in n- and p-type doped GaN layers which additionally enables to study their electroluminescence properties [13]. Hence, semipolar device structures can be grown on the c-plane of full 2" sapphire wafers, which are readily available and where high quality epitaxial growth is already well established.

In this paper, we like to review our recent studies about the epitaxial growth of such structures and their specific crystalline and optoelectronic characteristics. Moreover, LED devices have been processed showing reasonable properties. We will also discuss the viability of this approach for longer wavelength light emitters.

2 Epitaxial growth, device processing The fabrication of such facet based device structures requires two epitaxial steps. First, high quality GaN templates on c-plane sapphire were grown using an optimized procedure in low pressure MOVPE [14]. By conventional deposition, optical lithography, and dry etching techniques, SiO₂ mask stripes oriented along the {1 $\bar{1}$ 00} and {11 $\bar{2}$ 0} directions were deposited on these templates. Depending on the specific purpose, different mask designs have been used. Typical dimensions of the mask openings and mask periods ranged from 3 to 8 μ m and from 2 to 300 μ m, respectively.

Then, the samples have been taken back to the MOVPE reactor for the second epitaxial step. Now, the growth parameters were optimized to grow triangularly shaped n-doped GaN stripes in the mask openings formed by {11 $\bar{2}$ 2}



Figure 1 (online color at: www.pss-a.com) Schematic view on LED structures grown on the side facets of n-doped GaN stripes grown by selective area epitaxy using SiO₂ as mask material.

and {1 $\bar{1}$ 01} side facets develop for stripes running along the {1 $\bar{1}$ 00} and {11 $\bar{2}$ 0} directions, respectively, as described in more detail below. Thereon, we have typically grown 5 GaInN quantum wells followed by a GaN:Mg top layer (see Fig. 1). In order to get an appropriate In incorporation, the quantum wells as well as the GaN barriers between them were grown at a reduced temperature of about 800 °C, whereas all other layers have been typically grown at $T = 1020$ °C.

On our LED test structures, a simple device processing procedure was applied. Circular In p-contacts with diameters between 70 and 140 μ m were defined by standard lithography on the grown stripes without formation of mesa structures. The EL characteristics were measured on-wafer, collecting the light with an integrating sphere [15].

3 Theoretical expectations By assuming pseudo-morphically grown GaInN layers on unstrained GaN substrate, the strain situation in the quantum wells and the resulting piezoelectric field can be calculated. As pointed out by Takeuchi et al. in their pioneering work [4], the latter depends mainly – besides its strain dependence – on the angle between the respective facet normal and the c-direction. As compared to c-plane quantum wells, this leads to a reversed piezoelectric field with a magnitude of about 1/3 for our quantum wells formed on {11 $\bar{2}$ 2} and {1 $\bar{1}$ 01} side facets, which enclose an angle with the c-plane of 58 and 62°, respectively (Fig. 2).

This lower piezoelectric field leads to a substantially increased internal quantum efficiency in the quantum wells, which can be estimated by solving Schrödinger's equation for the tilted potential in the GaInN quantum well and calculating the overlap integrals of the two wave functions for electrons in the conduction band and holes in the valence band [17] (Fig. 3).

4 Structural characteristics of the stripes

4.1 General stripe structure By choosing the adequate growth conditions in selective area epitaxy, growth only takes place on the mask-free areas, fed by the precursor material supplied to the total area. The material arriving above the masked stripes is transported to the open areas by gas phase diffusion, as studied for the epitaxial growth of arsenides and phosphides (see, e.g., Ref. [18]). Consequently, the growth rate in the openings increases according to the respective ratio between the masked and open area [19].

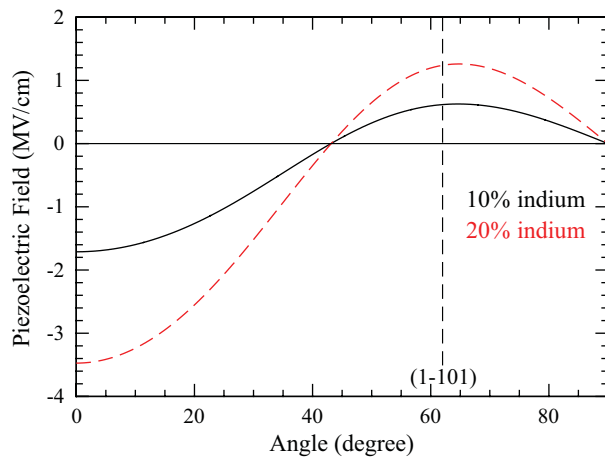


Figure 2 (online color at: www.pss-a.com) Calculated piezoelectric field for $\text{Ga}_{1-x}\text{In}_x\text{N}$ quantum wells grown pseudomorphically on unstrained GaN for different growth directions. Input data for these calculations from [16]. The angle θ is defined as angle between the $\langle 0001 \rangle$ direction and the actual growth direction.

In order to achieve exclusively semi-polar facets by selective area epitaxy, the growth process has to be adjusted so that the selectively grown stripes have triangular cross-section. For stripes running along the $\langle 1\bar{1}00 \rangle$ direction, depending on the growth conditions either a triangular cross-section with semi-polar $\{11\bar{2}\bar{2}\}$ facets or a rectangular shape can be established [12], where the side facets are completely non-polar a-plane facets. However, the rectangular shape requires polar c-plane facets on top, which is not favorable for our purpose. For stripes along $\langle 11\bar{2}0 \rangle$, triangular cross-sections with semi-polar $\{1\bar{1}01\}$ facets are obtained in a wide range of growth conditions. As mentioned above, we

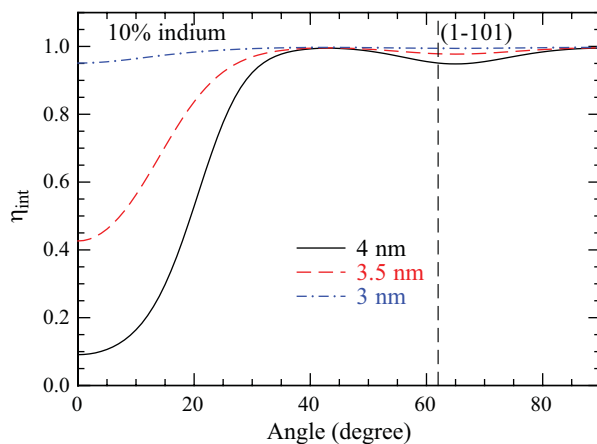


Figure 3 (online color at: www.pss-a.com) Calculated internal quantum efficiency η_{int} for $\text{Ga}_{0.9}\text{In}_{0.1}\text{N}$ quantum wells of different widths virtually grown in different crystal orientations (angle with respect to the c-direction). The $\langle 1\bar{1}01 \rangle$ direction is marked by a vertical dashed line. For all quantum well widths the same non radiative decay is assumed so that the internal efficiency of the 3 nm wide well in $\langle 0001 \rangle$ direction is 0.95.

have concentrated our studies on triangular cross-sections. However, for fairly wide openings, the triangular stripes may not develop completely resulting in stripes with trapezoidal cross-section, the top facet being a $\{0001\}$ or c-plane, and the local growth rate may depend on the facet type.

A detailed evaluation of the local growth rates indicated different growth rates on the different facet types. The quantum wells grown on the top c-plane facets of trapezoidal stripes grow much faster than those on the side facets, the details depending on the stripe direction [19]. This was further confirmed by locally resolved X-ray studies performed at the Cornell High Energy Synchrotron Source (CHESS) [20].

This behavior is reversed for the growth of the top p-doped GaN layer. Now, a thick layer grows on the facet, whereas only little growth takes place on the top c-planes. This is obviously a consequence of the fact that Mg-doping leads to strongly enhanced lateral growth [21]. The thin or even missing p-layer at the apex of our stripes may lead to short circuits of our devices when forming electrical contacts [22]. When an undoped GaN layer is grown on top under otherwise the same growth conditions, again the growth on the c-plane top facet is faster than on the side facets.

For pure triangular stripes, the two different $\{11\bar{2}\bar{2}\}$ and $\{1\bar{1}01\}$ side facets enclose nearly the same angle of about 58° and 62° with the c-plane, respectively. Therefore, a similar growth behavior can be expected. Indeed, the growth rates coincide quite well.

However, when we analyzed the composition of the quantum wells by measuring the integrated photoluminescence signal over a bunch of stripes [23], a significantly longer wavelength was found on triangular stripes running along the $\langle 11\bar{2}0 \rangle$ direction. Obviously, the incorporation of indium is more efficient on the $\{1\bar{1}01\}$ planes as compared to the $\{11\bar{2}\bar{2}\}$ planes [24].

The above mentioned locally resolved X-ray studies have additionally given some evidence for an increased In incorporation on $\{1\bar{1}01\}$ planes of triangular stripes as compared to unstructured c-planes [25]. This was further proven by growing about 50 nm thick GaInN layers which enabled standard X-ray diffraction analysis [26], indicating a 50% higher In incorporation efficiency. This tendency was predicted by Northrup et al. [27]. Similar observations have been reported for semipolar quantum wells grown on a $\{11\bar{2}\bar{2}\}$ facet [28]. The noticeable higher In incorporation should help significantly to achieve longer wavelength emission despite the reduced QCSE.

When comparing the surface flatness of the stripes running in the two main directions [29], we observed that the $\{1\bar{1}01\}$ side facets typically develop a much flatter surface with an RMS roughness measured by atomic force microscopy of about 0.25 nm [15], whereas the $\{11\bar{2}\bar{2}\}$ facets of the stripes running along $\langle 1\bar{1}00 \rangle$ show a rough surface with stripe-like features running from the top to the bottom. Moreover, the latter stripes typically develop a defective apex, whereas the other stripes have mostly perfect triangular cross-section. This may be related to the fact that

the $\{1\bar{1}01\}$ plane is a more natural crystal surface, as it typically develops on freely grown crystals [30]. This better facet quality forced us to concentrate our further studies on stripes with $\{1\bar{1}01\}$ side facets.

All these observations clearly demonstrate the influence of different interfacet diffusion processes of the involved atoms between the two semi-polar facets and their associated c-plane top facets besides gas-phase diffusion effects of the precursor molecules, which are mainly depending on the mask design.

Funato et al. have proposed to use these effects to realize LED structures with laterally different emission wavelength, eventually leading to multi-color or white light emitting devices by growing triangular, trapezoidal, and other stripes side by side using more complicated mask designs with locally different stripe geometries [31].

These studies, although not yet conclusively finished, shed light on the incorporation mechanisms of the metals in such an epitaxial process and hence may help to solve important questions about the incorporation efficiency of In into GaInN which is not following the mass transport limitations typically observed in MOVPE of similar materials like GaInAs or GaInP.

4.2 Local layer structure In addition to these differences for different facets and mask geometries, we have found, that both, the GaInN quantum well thickness and composition vary on one single facet when going from top to bottom. Cross-section micrographs obtained by transmission electron microscopy typically indicate an increase of the quantum well thickness near the stripe apex. The above mentioned locally resolved high resolution X-ray

measurements [25] show that the In content increases accordingly, which could be confirmed by locally resolved cathodoluminescence measurements (Fig. 4) and has been also observed by other groups [32, 33].

Nishizuka et al. [34] have found even stronger variations of the quantum wells' properties across $\{11\bar{2}2\}$ stripe facets. They used atmospheric pressure epitaxy [9] where the precursor diffusion lengths are shorter than at low pressure used in our experiments. Indeed, we observed a decrease in the linewidth of the GaInN photoluminescence line measured over several stripes when reducing the reactor pressure during the growth of the quantum wells from 300 to 100 hPa (Fig. 5) confirming these conclusions, although this effect may be less pronounced on $\{1\bar{1}01\}$ facets of stripes running along $\langle 11\bar{2}0 \rangle$, which are typically more uniform at higher pressures than those on $\{11\bar{2}2\}$ facets. Srinivasan et al. [35] proposed to use this effect for the realization of multi-color emitting devices using the latter facet stripes.

However, in some cases, this trend is reversed leading to long-wavelength emission at the bottom when scanning over a facet. This is also visible on our stripe displayed in Fig. 4. The final result seems to depend on the details of the mask geometry (size of masked area between stripes etc.) and may be an interplay of gas phase diffusion and surface migration of the respective constituents [33].

5 Optoelectronic properties Besides these structural properties, the reduced internal piezo-electric field is the main concern of growing such facet quantum wells. In order to measure directly this field, we have performed field-dependent photoluminescence experiments [36, 17]: An external reverse voltage is applied to a p-n-diode structure

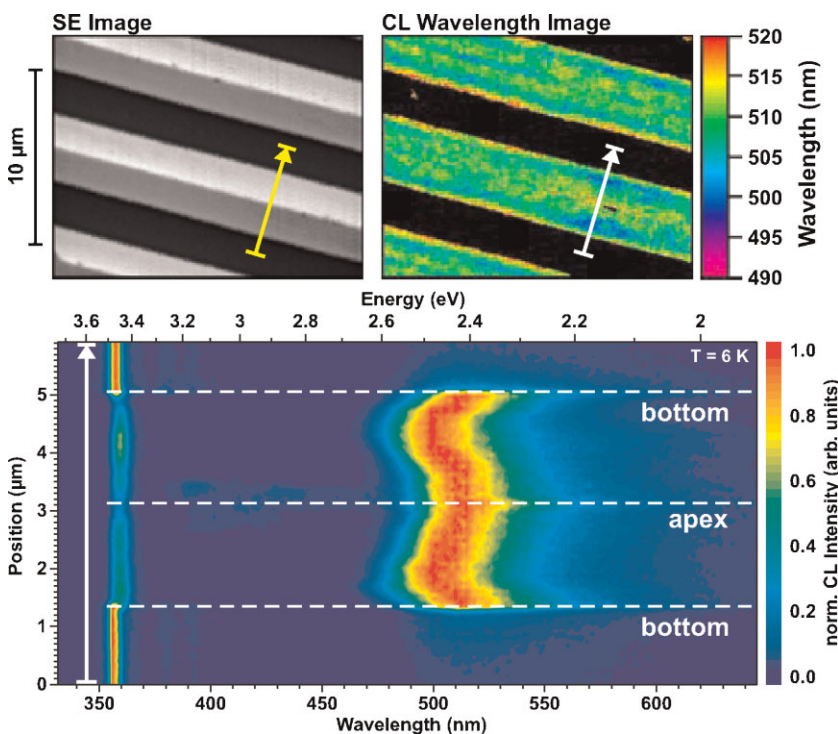


Figure 4 (online color at: www.pss-a.com) Low temperature cathodoluminescence scan over a stripe running along the $\langle 11\bar{2}0 \rangle$ direction (bottom) as indicated in the SEM micrograph (top left) and in the CL wavelength image (top right). The intensity of the spectra in the bottom diagram is color coded (see intensity scale at right end of diagram). The quantum well emission is visible at about 520 nm, whereas at about 356 nm, the GaN luminescence is visible.

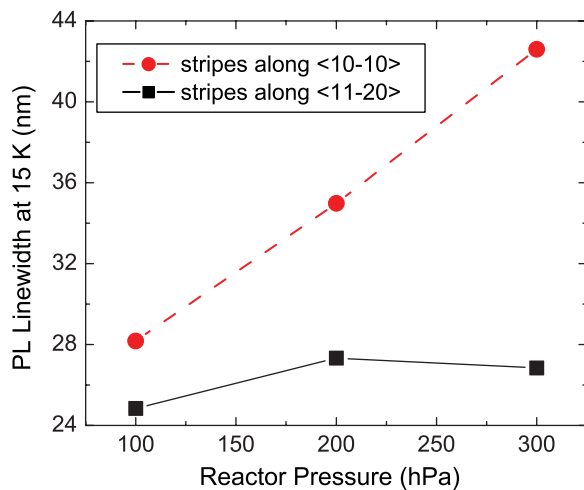


Figure 5 (online color at: www.pss-a.com) Full width at half maxima of low temperature photoluminescence spectra of quantum wells emitting at about 490 nm at different reactor pressures.

containing the embedded quantum well thus more or less compensating the internal field. By evaluating the simultaneously detected PL emission energy as a function of the applied voltage, a full fit allows to determine the piezoelectric field.

Evaluating the spectra [17], we find that flat band condition can be established for both, a polar and a non-polar sample within the applicable voltage range. Hence we could determine the electric field to be -1.84 MV/cm for our c-plane reference sample. For our semipolar facet, we evaluated an internal field of -120 kV/cm, which is smaller and of opposite sign than expected from Fig. 2. The discrepancy seems to be attributed to the particular local strain of the GaN stripe, which was not included in our evaluation procedure yet. A closer look to these effects is currently underway and will be published elsewhere. However, our measurements clearly prove the strong reduction of the internal piezoelectric field on our facets.

This could be further verified by time- and locally resolved PL measurements on our semipolar LED structures [37]. The stronger overlap of the electron and hole wave functions lead to a drastically reduced carrier recombination time of 650 ps at 4 K for the GaInN facet quantum wells as opposed to very long decay times of more than 50 ns for the c-plane reference sample.

Although both samples were grown under similar conditions, the structural properties of their active regions are expected to be slightly different. Taking into account the results discussed above and some other results including electron microscopy and photoluminescence data obtained on these particular samples, it is evident that the semipolar quantum wells are somewhat thicker and contain more In. As known from c-plane LEDs, both effects would increase the carrier lifetime [38]. Hence, the determined short decay time is definitely attributed to the reduced piezoelectric field in our facet quantum wells.

Moreover, the semipolar sample showed significantly stronger light intensity than the polar one over the investigated excitation power range [37] ruling out the influence of additional non-radiative defects. We could obtain fairly strong EL intensities on semipolar stripe LED test structures of 1 mW at 30 mA measured after simple device processing on wafer for devices emitting at 425 nm [22], although in particular the p-doping profile is still far from being optimized. Their PL and EL peak positions show a much weaker shift with excitation power, respectively current, of about 1/3 as compared to the reference [22, 37]. Such a shift indicates the screening of the internal field by higher carrier concentrations. This is in excellent agreement with our expectations (see Section 3) [39, 40] that the internal field is reduced by about the same factor in the semipolar samples.

6 Longer wavelength emission Such reduced internal fields should be most effective in long wavelength light emitters containing heavily strained GaInN quantum wells. However, owing to the reduced QCSE, non- or semipolar devices require even higher In contents as the respective polar structures to achieve the same emission wavelength. Hence, more problems related to the incorporation of indium into the epitaxial layer are expected.

Therefore, a careful optimization of the growth parameters of the GaInN quantum wells is required to shift the emission wavelength toward the green region. By lowering the growth temperature to 775 °C while optimizing growth rate and V-III ratio, we could obtain quantum wells containing about 28% In. Moreover, the growth of the subsequent p-region of the diode structure, typically performed at temperatures above 1000 °C, was optimized in order not to degrade these quantum wells.

Figure 6 (inset) shows the spectrum of a respective LED test structure at a driving current of 100 mA. A FWHM of 215 meV was determined at a wavelength of 495 nm. Optical output powers as high as 240 μ W@20 mA and 1 mW@110 mA have been measured on-wafer [15].

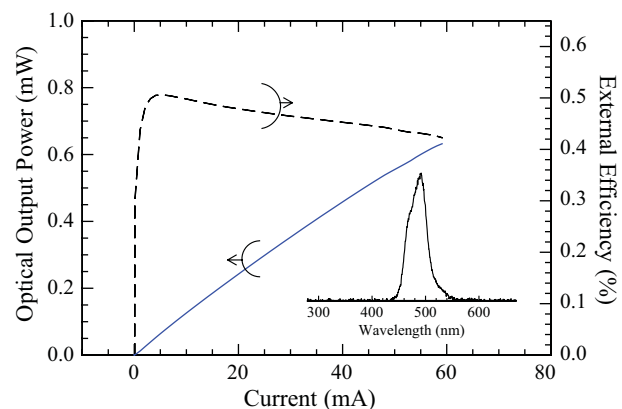


Figure 6 (online color at: www.pss-a.com) Optical output power and external efficiency of a semipolar facet LED emitting at 495 nm. The inset shows the spectrum of a LED measured at 100 mA.

Interestingly, the external efficiency stays nearly constant for the investigated current range (Fig. 6). This is believed to primarily result from the reduction of the piezoelectric field on the semipolar side facets.

In order to push the wavelength even more into the green region, we have further optimized several growth parameters to achieve a high In incorporation without surpassing the miscibility limit. As mentioned above, much higher In concentrations must be achieved for the same wavelength as compared to c-plane growth to compensate the reduced QCSE. Unfortunately, we did not yet find indications that the miscibility limit is shifted significantly to higher In concentrations on our semipolar facets. Similar to growth experiments for green emission on c-plane GaN [41], we obtained best results with low temperature, high V/III ratio and similar TEGa- und TMIn-precursor flows. Figure 7 (full red line) shows the PL spectrum at room temperature for an undoped semipolar GaInN/GaN multiple quantum well (MQW) structure emitting in the green spectral range. Fairly strong luminescence from the 3 GaInN MQWs containing about 32% In can be observed peaking at 518 nm.

7 Inverted pyramids The results presented above show that the light emission of our semipolar structures is still comparably weak. Besides our still not optimized device structures, particularly concerning the doping profiles etc., we think, that also the defect structure in our stripes may be responsible for the limited performance. We have observed that the threading dislocations from the template penetrate our stripes running along $\langle 11\bar{2}0 \rangle$ and hence are still present on the semipolar $\{1\bar{1}01\}$ facets. This is opposite to stripes running along $\langle 1\bar{1}00 \rangle$ where a bending of the dislocations from vertical to horizontal can be observed when lateral growth proceeds. This effect is most effective in defect reduction by the well-known facet-assisted epitaxial lateral overgrowth (FACELO) process [42, 43]. However, as

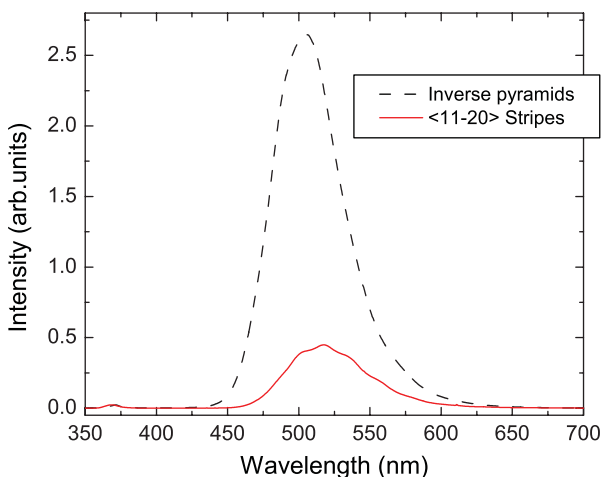


Figure 7 (online color at: www.pss-a.com) Room temperature PL spectra of undoped semipolar GaInN/GaN MQW structures. Full line: Quantum wells grown on the $\{1\bar{1}01\}$ side facets of stripes running along $\langle 11\bar{2}0 \rangle$ peaking at 518 nm. Broken line: Quantum wells grown on an inverted pyramid structure.

described above, the $\{11\bar{2}2\}$ facets on those stripes have inferior surface quality.

Therefore, we have recently started to investigate another approach: By defining masks with a honeycomb pattern where the center of each cell is masked and the surrounding is the window region, inverted pyramids can be obtained in selective area epitaxy [44]. In such structures, first $\{11\bar{2}2\}$ facets can be formed where the defects are bent horizontally. When overgrown further, eventually $\{1\bar{1}01\}$ facets develop with potentially very low defect density. Indeed, respective inverted pyramids where only GaN is grown show excellent properties in luminescence, evidenced by a strong donor bound exciton line with a FWHM of 2.6 meV at low temperature despite a still present slight strain variation over the facet. First GaInN quantum well structures grown on these inverted facets show indeed bright PL (Fig. 7, black broken line). However, locally resolved cathodoluminescence spectra indicate that the thickness and/or composition of these quantum wells is less uniform than on long stripes. More details will be published in Refs [45, 46].

8 Summary In order to obtain semipolar GaInN quantum wells on high quality c-plane GaN buffers, we have investigated the growth of such quantum wells on the side facets of triangular GaN stripes grown by selective area epitaxy. The predicted reduced piezoelectric field could be confirmed by several experimental methods. By carefully adjusting the growth conditions of quantum wells containing large amounts of In, we could obtain reasonable electroluminescence output powers at 495 nm. The photoluminescence peak emission could be shifted up to 518 nm demonstrating the potential for obtaining highly efficient green light emitters. For further defect reduction, we changed our mask geometry from stripes to honeycomb patterns which results in inverted pyramids after the selective area growth process. Quantum wells grown on these inverted pyramids show bright luminescence, although thickness and/or composition non-uniformities seem to be more severe than on stripes.

Acknowledgements The work described in this paper was a result of strong interactions and cooperations with different groups all over the world. In particular we would like to thank P. Michler and his team (University of Stuttgart), and A. Sirenko and his team (New Jersey Institute of Technology). Moreover, our thanks go to B. Neubert (now with Suss GmbH, Munich), P. Brückner (now with UMS, Ulm), I. Argut, J. Wang, J. Hertkorn, F. Lipski, S. Schwaiger, and M. Wiedemann (Ulm University) for technical assistance. The financial support by the Deutsche Forschungsgemeinschaft is gratefully acknowledged.

References

- [1] I. H. Ho and G. B. Stringfellow, Mater. Res. Soc. Symp. Proc. **449**, 871 (1997).
- [2] T. Matsuoka, MRS Internet J. Nitride Semicond. Res. **3**, 54 (1998).

- [3] F. Bernardini, V. Fiorentini, and D. Vanderbilt, *Phys. Rev. B* **56**, R10024 (1997).
- [4] T. Takeuchi, H. Amano, and I. Akasaki, *Jpn. J. Appl. Phys.* **39**, 413 (2000).
- [5] Y. Enya, Y. Yoshizumi, T. Kyono, K. Akita, M. Ueno, M. Adachi, T. Sumitomo, S. Tokuyama, T. Ikegami, K. Katayama, and T. Nakamura, *Appl. Phys. Express* **2**, 082101 (2009).
- [6] K. Fujito, S. Kubo, and I. Fujimura, *MRS Bull.* **34**, 313 (2009).
- [7] P. Waltereit, O. Brandt, M. Ramsteiner, R. Uecker, P. Reiche, and K. H. Ploog, *J. Cryst. Growth* **218**, 143(2000).
- [8] T. Takeuchi, S. Lester, D. Basile, G. Girolami, R. Twist, F. Mertz, M. Wong, R. Schneider, H. Amano, and I. Akasaki, *Proc. Int. Workshop on Nitride Semiconductors, IPAP Conf. Series 1*, 137 (2000).
- [9] K. Nishizuka, M. Funato, Y. Kawakami, S. Fujita, Y. Narukawa, and T. Mukai, *Appl. Phys. Lett.* **85**, 3122 (2004).
- [10] S. Khatsevich, D. H. Rich, X. Zhang, W. Zhou, and P. D. Dapkus, *J. Appl. Phys.* **95**, 1832 (2004).
- [11] F. Scholz, T. Wunderer, B. Neubert, M. Feneberg, and K. Thonke, *MRS Bull.* **34**, 328 (2009).
- [12] K. Hiramatsu, K. Nishiyama, A. Motogaito, H. Miyake, Y. Iyechika, and T. Maeda, *Phys. Status Solidi A* **176**, 535 (1999).
- [13] B. Neubert, F. Habel, P. Brückner, F. Scholz, T. Riemann, and J. Christen, *Mater. Res. Soc. Symp. Proc.* **831**, E11.32.1 (2005).
- [14] J. Hertkorn, P. Brückner, S. B. Thapa, T. Wunderer, F. Scholz, M. Feneberg, K. Thonke, R. Sauer, M. Beer, and J. Zweck, *J. Cryst. Growth* **308**, 30 (2007).
- [15] T. Wunderer, F. Lipski, J. Hertkorn, P. Brückner, F. Scholz, M. Feneberg, M. Schirra, K. Thonke, A. Chuvilin, and U. Kaiser, *Phys. Status Solidi C* **5**, 2059 (2008).
- [16] H. Shen, M. Wraback, H. Zhong, A. Tyagi, S. P. DenBaars, S. Nakamura, and J. S. Speck, *Appl. Phys. Lett.* **95**, 033503 (2009).
- [17] M. Feneberg, F. L. M. Schirra, R. Sauer, K. Thonke, T. Wunderer, P. Brückner, and F. Scholz, *Phys. Status Solidi C* **5**, 2089 (2008).
- [18] E. J. Thrush, J. P. Stagg, M. A. Gibbon, R. E. Mallard, B. Hamilton, J. M. Jowett, and E. M. Allen, *Mater. Sci. Eng. B* **21**, 130 (1993).
- [19] B. Neubert, GaInN/GaN LEDs auf semipolaren Seitenfacetten mittels selektiver Epitaxie hergestellter GaN-Streifen, Ph.D. thesis, Universität Ulm (2008).
- [20] S. M. O'Malley, P. Bonanno, T. Wunderer, P. Brückner, B. Neubert, F. Scholz, A. Kazimirov, and A. A. Sirenko, *Phys. Status Solidi C* **5**, 1655 (2008).
- [21] W. V. Lundin, A. E. Nikolaev, A. V. Sakharov, and A. F. Tsatsul'nikov, *Semiconductors* **42**, 232 (2008).
- [22] T. Wunderer, P. Brückner, B. Neubert, F. Scholz, M. Feneberg, F. Lipski, M. Schirra, and K. Thonke, *Appl. Phys. Lett.* **89**, 041121 (2006).
- [23] B. Neubert, P. Brückner, F. Habel, F. Scholz, T. Riemann, J. Christen, M. Beer, and J. Zweck, *Appl. Phys. Lett.* **87**, 182111 (2005).
- [24] B. Neubert, F. Habel, P. Brückner, F. Scholz, M. Schirra, M. Feneberg, K. Thonke, T. Riemann, J. Christen, M. Beer, J. Zweck, G. Moutchnik, and M. Jetter, *Phys. Status Solidi C* **3**, 1587 (2006).
- [25] P. L. Bonanno, S. M. O'Malley, A. A. Sirenko, A. Kazimirov, Z. Cai, T. Wunderer, P. Brückner, and F. Scholz, *Appl. Phys. Lett.* **92**, 123106 (2008).
- [26] T. Wunderer, J. Hertkorn, F. Lipski, P. Brückner, M. Feneberg, M. Schirra, K. Thonke, I. Knoke, E. Meissner, A. Chuvilin, U. Kaiser, and F. Scholz, *Gallium Nitride Materials and Devices III*, edited by H. Morkoc et al., *Proc. SPIE* **6894**, 68940V-1 (2008).
- [27] J. E. Northrup, L. T. Romano, and J. Neugebauer, *Appl. Phys. Lett.* **74**, 2319 (1999).
- [28] P. De Mierry, T. Guehne, M. Nemoz, S. Chenot, E. Beraudo, and G. Nataf, *Jpn. J. Appl. Phys.* **48**, 031002 (2009).
- [29] B. Neubert, T. Wunderer, P. Brückner, F. Scholz, M. Feneberg, F. Lipski, M. Schirra, and K. Thonke, *J. Cryst. Growth* **298**, 706 (2007).
- [30] M. Aoki, H. Yamane, M. Shimada, S. Sarayama, H. Iwata, and F. J. Disalvo, *Jpn. J. Appl. Phys.* **42**, 5445 (2003).
- [31] M. Funato, T. Kutani, T. Kondou, Y. Kawakami, Y. Narukawa, and T. Mukai, *Appl. Phys. Lett.* **88**, 261920 (2006).
- [32] W. Feng, V. V. Kuryatkov, A. Chandolu, D. Y. Song, M. Pandikunta, S. A. Nikishin, and M. Holtz, *J. Appl. Phys.* **104**, 103530 (2008).
- [33] H. Fang, Z. J. Yang, Y. Wang, T. Lai, L. W. Sang, L. B. Zhao, T. J. Yu, and G. Y. Zhang, *J. Appl. Phys.* **103**, 014908 (2008).
- [34] K. Nishizuka, M. Funato, Y. Kawakami, Y. Narukawa, and T. Mukai, *Appl. Phys. Lett.* **87**, 231901 (2005).
- [35] S. Srinivasan, M. Stevens, F. Ponce, and T. Mukai, *Appl. Phys. Lett.* **87**, 131911 (2005).
- [36] M. Feneberg and K. Thonke, *J. Phys.: Condens. Matter* **19**, 403201 (2007).
- [37] T. Wunderer, P. Brückner, J. Hertkorn, F. Scholz, G. J. Beirne, M. Jetter, P. Michler, M. Feneberg, and K. Thonke, *Appl. Phys. Lett.* **90**, 171123 (2007).
- [38] F. Scholz, *Prog. Cryst. Growth Charact.* **35**, 243 (1997).
- [39] A. E. Romanov, T. J. Baker, S. Nakamura, J. S. Speck, and E. U. Group, *J. Appl. Phys.* **100**, 023522 (2006).
- [40] M. Feneberg, F. Lipski, R. Sauer, K. Thonke, T. Wunderer, B. Neubert, P. Brückner, and F. Scholz, *Appl. Phys. Lett.* **86**, 242112 (2006).
- [41] D. Fuhrmann, U. Rossow, C. Netzel, H. Bremers, G. Ade, P. Pinze, and A. Hangleiter, *Phys. Status Solidi C* **3**, 1966 (2006).
- [42] O. Nam, M. D. Bremser, T. S. Zheleva, and R. F. Davis, *Appl. Phys. Lett.* **71**, 2638 (1997).
- [43] K. Hiramatsu, K. Nishiyama, M. Onishi, H. Mizutani, M. Narukawa, A. Motogaito, H. Miyake, Y. Iyechika, and T. Maeda, *J. Cryst. Growth* **221**, 316 (2000).
- [44] T. Wunderer, F. Lipski, S. Schwaiger, J. Hertkorn, M. Wiedenmann, M. Feneberg, and K. T. F. Scholz, *Jpn. J. Appl. Phys.* **48**, 060201 (2009).
- [45] T. Wunderer, J. Wang, F. Lipski, S. Schwaiger, A. Chuvilin, U. Kaiser, S. Metzner, F. Bertram, J. Christen, S. S. Shirokov, A. E. Yunovich, and F. Scholz, *Phys. Status Solidi C* **7**, No. 7-8 (2010), these proceedings.
- [46] S. Metzner, F. Bertram, and J. Christen, to be published.